CrystEngComm

Accepted Manuscript

ROYAL SOCIETY OF CHEMISTRY

www.rsc.org/crystengcomm

Intermolecular Interaction influenced Energy and Sensitivity of High Energetic Salts: Structure and Physicochemical Property

Zhiyong Su,[a#] Xiangyu Liu, [a,b#] Qi Yang, [a] Sheng Zhang, [a] Qing Wei, [a] Gang Xie, [a] Sanping Chen, [a*] Shengli Gao [a]

[a] *Key Laboratory of Synthetic and Natural Functional Molecule Chemistry of Ministry of Education, College of Chemistry and Materials Science, Northwest University, Xi'an 710069, China*

[b] *School of Chemistry and Chemical Engineering, Ningxia University, Yinchuan 750021, China*

[#] *These authors contributed equally to this work.*

***Corresponding author**

Prof. Sanping Chen

Tel.: +8602988302604

Fax: +8602988302604

E-mail: sanpingchen@126.com

Abstract

Based on supramolecular interactions, three stable energetic compounds, $(TATA^{+})\cdot(TZA^{-})\cdot H_2O$ (**1**), $(AT^{+})_2\cdot(OX^{2-})$ (**2**), $(DAT^{2+})\cdot(NO_3^{-})_2$ (**3**), possessing nitrogen contents of 51.42%, 53.80 and 43.53%, respectively, were synthesized and structurally characterized (TATA = 1,3,5-triazine-2,4,6-triamine, TZA = tetrazole-1-acetic, AT = 5-amino-1H-tetrazole, OX = oxalic acid, DAT = 3,5-diamino-1,2,4-triazole). The physicochemical properties of the title compounds were theoretically and experimentally investigated in detail. Thermogravimetry and Density Functional Theory (DFT) calculation indicate that three energetic compounds show superior thermal stability. The non-isothermal thermokinetics parameters were also obtained by Kissinger's and Ozawa's methods. In addition, the standard molar enthalpies of formation were calculated from the determination of constant-volume combustion energies. As energetic materials, the detonation performances of compounds are discussed with combination of low sensitivity and environmentally friendly.

Key words: Energetic materials / Heterocycles / Detonation performance / Intermolecular interaction / Sensitivity / DFT

1. Introduction

Energetic materials include explosives, propellants, and pyrotechnics that are used for a variety of military purposes and civilian applications.[1] Classical energetic materials such as TNT (2,4,6-trinitrotoluene),[2] RDX (1,3,5-trinitro-1,3,5-triazine)[3] and HMX (1,3,5,7-tetranitro-1,3,5,7-tetrazocine) [4] gain their energy from oxidation of the carbon backbones [5] Unfortunately, Safety and high energy are always in conflict.[6] A large of new energetic materials have emerged recently in order to meet the challenging requirements and improve the performance of existing energetic materials.[7] The key requirements include tailored performance, insensitivity, stability, vulnerability and environmental safety.[8] As known, the detonation property of energetic materials depends mainly on their heat of formation, density and oxygen balance (composition), of which the former two are governed to some extent by the molecular structure.[9] The weak interactions such as hydrogen-bonding and π-π stacking interaction can be the important source to stabilize the molecular structure except for covalent bond.[10] Meanwhile, the intermolecular interactions can counteract the detonation performance and high sensitivity contradiction in the solid state.[11] Moreover, the new energetic materials should be easy to synthesize as well as storable for long periods.[12]

Nitrogen-rich energetic salts, as a kind of the high-energy density materials (HEDMs),[13] have attracted considerable interest due to their environmentally friendly[14] and relatively modest performance characteristics.[8] Not only salt formed is used to stabilize the materials through the formation of hydrogen-bond networks and so on, but also such compounds tend to display lower vapor pressures and higher densities than their atomically similar non-ionic derivatives.[15] High nitrogen-containing heterocycles such as pyrazole, imidazole, triazole, tetrazole, triazine and tetrazine are used to synthesize energetic salts, as a result of theirs conjugated structure as well as hydrogen bond acceptor and donor.[16] Therein, the most popular triazoles and tetrazoles derivatives possess the large number of inherently energetic N–N and C–N bonds. In energetic salts, triazoles and tetrazoles groups are used as cations, when nitrate, perchlorate, dinitramide energetic groups are often selected as appropriate anion, which not only reduces the detonation capacity as small as possible, but also improves the oxygen balance and provides the hydrogen bond donor and acceptor.

Based on the above, three new energetic compounds, $(TATA^{+})\cdot(TZA^{-})\cdot H_2O$ (**1**), $(AT^{+})_2\cdot(OX^{2-})$ (**2**), $(DAT^{2+})\cdot(NO_3^{-})_2$ (**3**), were synthesized and structurally characterized in the present work.

Three compounds exhibit stabilized structures due to the existence of abundance intermolecular interactions. Particularly, comparing with the analogues reported previously, [17] compound **3** shows a rarely structure in which one DAT is embraced with two nitrate anions in the asymmetric unit. The stability of the compounds was characterized by TG, DSC and DFT calculation. The standard molar enthalpies of formation were calculated from the determination of constant-volume combustion energies. Detonation performance (P, D, ΔH_{det}) were calculated with the main detonation product of environmental friendly molecular N_2. Sensitivity test shows that the compounds are insensitive to external stimulus. In a word, it is meaningful attempt to synthesize high energy and insensitivity materials.

2. Experimental

General caution: the compounds are energetic materials and tend to explode under certain conditions. Appropriate safety precautions (safety glasses, face shields, leather coat and ear plugs) should be taken, especially when the compounds are prepared on a large scale.

2.1. Materials and instruments

Chemical reagents and solvents were purchased commercially and used as received without further purification.

Elemental analyses were performed on a Vario EL III analyzer fully automated trace element analyzer. FT-IR spectra were recorded on a Bruker FTIR instrument as KBr pellets. Differential scanning calorimetry (DSC) and thermogravimetric analysis (TGA) were carried out on a Netzsch STA 449C instrument and a CDR-4P thermal analyzer of Shanghai Balance Instrument factory, respectively, using dry oxygen-free nitrogen as the atmosphere, with a flowing rate of 10 mL min^{-1}. About 0.5 mg sample was sealed in aluminum pans in the temperature range of 25-500 ^{o}C for DSC experiments. The sensitivity to impact stimuli was determined by fall hammer apparatus applying standard staircase method using a 2 kg drop weight and the results were reported in terms of height for 50% probability of explosion ($h_{50\%}$).[18] The friction sensitivity was determined on a Julius Peter's apparatus by following the BAM method.[19] The phase purity of the bulk samples were verified by X-ray powder diffraction (PXRD) measurements performed on a Rigaku RU200 diffractometer at 60 kV, 300 mA and Cu K_α radiation (λ = 1.5406 Å), with a scan speed of 5° min^{-1} and a step size of 0.02° in 2θ. DFT method in Gaussian 03 package was used to optimize

the structures.[20] The constant-volume combustion energies of the compounds were determined with a precise rotating-bomb calorimeter (RBC-type II). [21]

2.2.1. Preparation of $(TATA^{+})\cdot(TZA^{-})\cdot H_2O$ (1)

TATA (126mg, 1 mmol) was added to mixed solvent of water and ethanol (3:1, 20 mL) of TZA (128 mg, 1 mmol) with stirring at 80°C. The resulting solution was filtered and kept at room temperature for crystallization. After 3 days, colorless block crystals of **1** were obtained in a yield of 76% (based on TZA). Anal. Calcd. For $C_6H_{12}N_{10}O_3$ (272.26): C, 26.45; H, 4.41; N, 51.42. Found: C, 26.44; H, 4.39; N, 51.36. IR (KBr ,cm^{-1}): 3673s, 3526s, 3441s, 3103w, 1683m, 1629m, 1441s, 1387w, 1187w, 1113w, 985w, 801w, 566s.

2.2.2. Preparation of $(AT^{+})_2\cdot(OX^{2-})$ (2)

$OX\cdot 2H_2O$ (126 mg, 1mmol) and AT (170 mg, 2 mmol) were mixed in15 mL aqueous solution with stirring at 60 °C. The resulting solution was filtered and kept at room temperature for crystallization. After 3 days, colorless block crystals of **2** were obtained in a yield of 81% (based on AT). Anal. Calcd. For $C_4H_8N_{10}O_4$ (260.20): C, 18.45; H, 3.07; N, 53.80. Found: C, 18.41; H, 3.05; N, 53.66. IR (KBr, cm^{-1}): 3675s, 3524s, 3443s, 3270w, 1743w, 1677w, 1582m, 1413w, 1246m, 1061w, 995w, 869w, 721m , 557s.

2.2.3. Preparation of $(DAT^{2+})\cdot(NO_3^{-})_2$ (3)

DAT (495mg 4 mmol) was added to nitric acid solution (4 mL, 16 mmol, 4 M) with stirring at room temperature. The resulting solution was filtered and kept at room temperature for crystallization. After 3 days, colorless block crystals of **3** were obtained in a yield of 78% (based on DAT). Anal. Calcd. For $C_2H_7N_7O_6$ (225.15): C, 10.66; H, 3.11; N, 43.53. Found: C, 10.63; H, 3.08; N, 43.45. IR (KBr,cm^{-1}): 3436s, 3346m, 3271m, 3162m, 2985w, 2762w, 1696s, 1678s, 1613m, 1540m, 1410m, 1335s, 1244m, 1140m, 1055w, 809w, 790w, 716w, 676w.

2.3. X-ray structure determinations

For **1**, **2** and **3**, selected single crystals were performed on a Bruker Smart Apex CCD diffractometer equipped with graphite monochromatized Mo *K*α radiation (λ = 0.71073 Å) using ω and φ scan modes. The single-crystal structures were solved by direct methods using SHELXS-97 [22] and refined by means of full-matrix least-squares procedures on F^2 with SHELXL-97[23] program. All non-H atoms were located using subsequent Fourier-difference methods and refined anisotropically. In all cases hydrogen atoms were placed in calculated positions and thereafter

allowed to ride on their parent atoms. Other details of crystal data, data collection parameters and refinement statistics were given in Table 1. Selected bond lengths and bond angles of title compound were listed in Table S1 (Supporting information). Hydrogen bonding parameters were listed in Table S2 (Supporting information). CCDC 969657 for 1, 969658 for 2 and 976693 for 3 contain the supplementary crystallographic data for this paper. These data can be obtained free of charge from The Cambridge Crystallographic Data Centre via www. ccdc. cam. ac. uk/ data _ request /cif.

Table 1

3. Results and discussion

3.1. Structure description

*3.1.1. X-ray structure of $(TATA^{+})\cdot(TZA^{-})\cdot H_2O$ (**1**)*

Structure determination reveals that the crystal structure of **1** consists of one TATA, TZA and one water molecule in the asymmetric unit (Fig 1a). Both TATA and TZA molecules are surrounded by extensive hydrogen bonds. A pair of TATA ions are dimerized through two N–H···N hydrogen bonds [N10···N7, 3.047(4), N5···N9 3.016(4) Å] similar to those observed in TMP sorbate, TMP-o-nitrobenzoate complexes (TMP) trimethoprim,[24] forming 1D chain (red rectangular box in Figure 1d). It is noteworthy that the water molecule forms two donor hydrogen bonds O–H···O [O1···O3 2.773(4), O1···O2A 2.754(4) Å] with two carboxylate oxygen atoms from two TZA ions and two acceptor hydrogen bonds N–H···O [N5···O1 3.095(4), N6···O1 2.707(4) Å] with one Tata $^{+}$ ion (Figure 1b). Furthermore, one carboxylate group in TZA anion is hydrogen bonded with two adjacent TATA cations in the 1D chain [N5···O3 2.849(4), N8A···O3 2.830(4) Å]. N2 and N4 atoms of each TZA ion are associated with two TATA cations from another chain to form hydrogen bonds N–H···N [N10···N4 2.939(4), N8···N2 3.022(4) Å] (Figure 1c), further leading to 2D layers. Finally, these sheets are stacked into complicated 3D hydrogen bonds network structure with the aids of free water molecules (Figure 1d).

Figure 1

*3.1.2. X-ray structure of $(AT^{+})_2\cdot(OX^{2-})$ (**2**)*

Compound **2** crystallizes in a monoclinic system *P*2(1)/*c*. The unit cell contains two chemical units composed of two AT molecules and one molecule of oxalic acid. The AT molecules are approximately coplanar with the OX molecules (dihedral angle 18.67°). The carboxylic groups in OX are linked with four AT molecules through hydrogen bonds N–H···O. The cations within each chain are interconnected by the N–H···N hydrogen bond (N1···N5 3.184(5) Å). The AT molecules are connected with the OX molecules to produce a 2D hydrogen-bonding network. The AT cation rings show face-to-face alignment and the separated interplanar center-to-center distances of 3.6377(10) Å (Figure 2b). The 3D structure is formed based on hydrogen-bonding and π-π type interaction (Figure 2c). Hydrogen-bonding parameters are detailed in Table S2 (Supporting information).

Figure 2

3.1.3. X-ray structure of $(DAT^{2+})\cdot(NO_3^-)_2$ (***3***)

In **3**, the asymmetric unit contains two nitrate anions and one DAT cation (Figure 3a) compared to the compound in reference [17]. Each DAT cations interact with six nitrate anions in the compound (Figure 3b). Furthermore, all oxygen atoms in the nitrate anions and all nitrogen atoms in the DAT cations form strong N–H···O hydrogen bonds. The structure of **3** is built on the basis of the layers containing the nitrate anions and the DAT cations, see Figure 3c. Hydrogen-bonding parameters are listed in Table S2 (Supporting information).

Figure 3

3.2. Thermal decomposition

The thermal behaviors of **1–3** were determined, using DSC and TG measurements with the linear heating rate of 5 °C min^{-1} under nitrogen atmosphere. In order to confirm the phase purity of the compounds, X-ray powder diffraction (PXRD) experiments have been carried out (Fig S1). The experimental patterns are in good agreement with the simulated, indicating the phase purity of the as-synthesized powder products. DSC and TG curves of these energetic salts are depicted in Figures 4 and 5.

As shown in Figure 4, compound **1** shows three main peaks. The first endothermic peak is a dehydration process, while the exothermic peak indicates the main decomposition reaction. The second endothermic peak is attributed to the condensation reaction of the residual fragments. For **2**, the exothermic peak represents the main decomposition, when the endothermic peak reflects the condensation reaction of the residual fragments. For **3**, there are two endothermic and one exothermic processes. The first endothermic peak corresponds to a phase transition, the exothermic peak shows the main decomposition process, and the second endothermic peak represents the condensation reaction of the residual fragments.

Figure 4

TG study for compound **1** shows that the first process accompanies a weight loss of 6.56% in the temperature range 140–160 °C, which is close to the theoretical calculation value of 6.61% for the loss of water molecules. The second process shows about 48.75% weight loss in the temperature range 246–300 °C, the weight loss is mainly caused by the breaking of TATA (Calcd. 46.28%). Followed that, the third process accompanies about 40.32% weight loss in the temperature range 300–500 °C attributed to condensation reaction of the residual fragments. For **2**, the decomposition process occurs at 185 °C, which corresponds to the collapse of framework and decomposition of organic components, accompanying the weight loss about 97.83% up to 500 °C. For **3**, the decomposition process with the weight loss about 98.21% corresponds to the collapse of framework and decomposition of organic components in the temperature range of 245–500 °C, showing that there decompose residual free for compounds **2** and **3**.

Figure 5

3.3. Optimized structure, total energy and the frontier orbital energy (hartree)

The crystal asymmetric units of the compounds were selected as the initial structure, and the DFT-B3LYP/6-31+G(d) method was used to optimize the structure of the compounds and compute their frequencies. Vibration analysis indicates that the optimized structure are in accordance with the minimum points on the potential energy planes, which means no virtual

frequencies, proving that the obtained optimized structures are stable.

Molecular total energy (E_{total}), frontier orbital energy levels (E_{HOMO} and E_{LUMO}), and their gaps (ΔE) are –1009.093700, –0.20474, –0.04917, and 0.15557 hartree for **1**, –1005.676573, –0.26431, –0.05580 and 0.20851 hartree for **2**, –914.885282, –0.24741, –0.06978 and 0.17763 hartree for **3**. The large value of ΔE can be as an important parameter to express the stability of the energetic materials. [25] According to the MO theory, HOMO and LUMO are the most important factors that affect the property of the compounds. The view of HOMO and LUMO are shown in Figures 6–8. For **1**, the electron density of HOMO mainly focuses on TZA, while that of LUMO focuses on TZA and TATA. For **2**, the electron density of OX in HOMO is lower than that in LUMO, while AT almost stays the same in both states. For **3**, the electron density of HOMO is mainly focused on DAT, while that of LUMO are mainly focused on DAT and one NO_3^-.

Figure 6

Figure 7

Figure 8

3.4. Non-isothermal kinetics analysis for the exothermal process

In our present work, Kissinger's method [26] and Ozawa's method [27, 28] are used to determine the apparent activation energy (E) and the pre-exponential factor (A). The Kissinger equation (1) and Ozawa equation (2) are as follows, respectively:

$$\ln(\frac{\beta}{T_p^2}) = \ln\frac{AR}{E} - \frac{E}{R}\frac{1}{T_p} \quad (1)$$

$$\log\beta + \frac{0.4567E}{RT_p} = C \quad (2)$$

Where A is the pre-exponential factor; E is the apparent activation energy; T_p is the peak temperature; R is the gas constant, 8.314 J mol^{-1} °C^{-1}; β is the linear heating rate and C is constant.

Based on the exothermic peak temperatures measured at four different heating rates of 2, 5, 8, 10 °C min^{-1}, Kissinger's and Ozawa–Doyle's method are applied to study the thermokinetics

parameters for the exothermal processes in compounds **1-3**. From the original data, we can achieve the apparent activation energy E_k and E_o, pre-exponential factor A_k and linear correlation coefficients R_k and R_o, as shown in Table 2.

Table 2

From Table 2, it is obvious that T_p of the exothermic peak shift to higher temperatures as the heating rate increases. E calculated from the Kissinger method (E_K) agrees well with that obtained by Ozawa's method (E_o). Besides, these linear correlation coefficients are very close to 1 and it is thus predicted that the results are credible. The Arrhenius Equations can be expressed as follows (E is the average of E_k and E_o): $\ln k = 59.024 - 614.29\times10^3/(RT)$ for **1**, $\ln k = 13.584 - 139.62\times10^3/(RT)$ for **2**, $\ln k = 13.160 - 152.84\times10^3/(RT)$ for **3**, respectively, which can be used to estimate the rate constant of the main step of thermal decomposition process of the compounds.

3.5. Oxygen-Bomb calorimetry

The constant-volume combustion energies of the compounds were determined with a precise rotating-oxygen bomb calorimeter (RBC-type II). [21] Approximately 200 mg of the samples were pressed with a well-defined amount of benzoic acid (Calcd. 800 mg) to form a tablet to ensure better combustion. The recorded data are the average of six single measurements. The calorimeter was calibrated by the combustion of certified benzoic acid (SRM, 39i, NIST) in an oxygen atmosphere at a pressure of 30.5 bar.

The experimental results for the constant volume combustion energies ($\Delta_c U$) of energetic compounds **1–3** are –16759.16 ± 6.12, –11961.22 ± 5.28 and –6451.57 ± 3.86 J g^{-1}, respectively. On the basis of the formula $\Delta_c H_m^\theta = \Delta_c U + \Delta nRT$, $\Delta n = n_g$(products, g) – n_g(reactants, g), (n_g is the total molar amount of gases in the products or reactants, R = 8.314 J mol^{-1} K^{-1}, T = 298.15 K), the standard molar enthalpies of combustion ($\Delta_c H_m^\theta$) can be derived as being –4554.17 ± 1.67 kJ mol^{-1} for **1**, –3112.31 ± 1.375 kJ mol^{-1} for **2**, –1440.795 ± 0.87 kJ mol^{-1} for **3**. The combustion reaction equations are listed as follows:

$C_6H_{12}N_{10}O_3$ (s) (**1**) + 7.5 O_2 (g) = 6 CO_2 (g) + 6 H_2O (l) + 5 N_2 (g) (3)

$C_4H_8N_{10}O_4$ (s) (**2**) + 4 O_2 (g) = 4 CO_2 (g) + 4 H_2O (l) + 5 N_2 (g) (4)

$C_2H_7N_7O_6$ (s) (**3**) + 0.75 O_2 (g) = 2 CO_2 (g) + 3.5 H_2O (l) + 3.5 N_2 (g) (5)

The standard molar enthalpies of formation of the combustion products CO_2 (g), $\Delta_f H_m^\theta$ (CO_2, g) = (–393.51 ± 0.13) kJ mol^{-1}, H_2O (l), $\Delta_f H_m^\theta$ (H_2O, l) = (–285.830 ± 0.040) kJ mol^{-1} were obtained from literature [29]. According to Hess's law, the standard molar enthalpies of formation ($\Delta_f H_m^\theta$) of **1**–**3** at 298.15 K are calculated as being 478.13 ± 1.78, 382.56 ± 3.51 and –346.63 ± 2.45 kJ mol^{-1}, respectively.

3.6. Heat of detonation

According to the order of H_2, CO, C or H_2, CO, CO_2 in forming detonation products, [30] the detonation products of **1**, **2** and **3** are calculated as follows:

$$C_6H_{12}N_{10}O_3 = 6\ H_2 + 3\ CO + 3\ C + 5\ N_2 \quad (6)$$

$$C_4H_8N_{10}O_4 = 4\ H_2 + 4\ CO + 5\ N_2 \quad (7)$$

$$C_2\ H_7N_7O_6 = 3.5\ H_2O + 1.5\ CO + 0.5\ CO_2 + 3.5\ N_2 \quad (8)$$

To estimate the heat of detonation of the compounds, Density functional theory (DFT) was used to compute the energy of detonation (ΔE_{det}), where ΔH_{det} is estimated by using a linear correlation equations (ΔH_{det} = 1.127 ΔE_{det}+ 0.046, r = 0.968).[31] The calculated values of ΔE_{det} and ΔH_{det} are listed in Table 3.

Table 3

From Table 3, the heat of detonation of compound **1** is calculated to be 4.2594 kcal g^{-1}, which is far higher than those of TNT and RDX.

3.7. Characterization of detonation velocity and pressure

Detonation velocity (D) and detonation pressure (P) are the most important parameters of the detonation characteristics of energetic materials. The detonation products produced by general explosives together with their nitrogen equivalent indices are listed in Table 4.

Table 4

The values of D and P of an explosive can be predicted with the nitrogen equivalent equation (NE equation) shown as formulas (9)–(11) [32]

$$\sum N = 100 \sum \frac{X_i N_i}{M} \quad (9)$$

$$D = (690 + 1160\,\rho_0) \sum N \quad (10)$$

$$P = 1.092\,(\rho_0 \sum N)^2 - 0.574 \quad (11)$$

where ρ_0 represents density of an explosive; M represents molecular mass of an explosive; $\sum N$ represents nitrogen equivalent of the detonation products; N_i represents nitrogen equivalent index of certain detonation product; X_i represents the mole number of certain detonation product produced by a mole explosive.

According to Eqs (6), (7), (8) and (9), in which M(**1**) = 272.26 g mol^{-1}, M(**2**) = 260.20 g mol^{-1} and M(**3**) = 225.15 g mol^{-1}, total nitrogen equivalents of **1**, **2** and **3** are calculated through the nitrogen equivalent indexes of the detonation products. As follows:

$$\sum N1 = \frac{100 \times (6 \times 0.29 + 3 \times 0.78 + 3 \times 0.15 + 5 \times 1)}{272.26} = 3.50$$

$$\sum N2 = \frac{100 \times (4 \times 0.29 + 4 \times 0.78 + 5 \times 1)}{260.20} = 3.57$$

$$\sum N3 = \frac{100 \times (3.5 \times 0.54 + 1.5 \times 0.78 + 0.5 \times 1.35 + 3.5 \times 1)}{225.15} = 3.21$$

According to Eqs. (10) and (11), in which ρ_0(**1**) = 1.551 g cm^{-3}, ρ_0(**2**) = 1.651g cm^{-3} and ρ_0(**3**) = 1.842 g cm^{-3}, D and P can be obtained as follows:

D**1** = (690 + 1160ρ_{01}) $\sum N$**1** = (690+1160 × 1.551) × 3.50 = 8712.06 m s^{-1}

D**2** = (690 + 1160ρ_{02}) $\sum N$**2** = (690+1160 × 1.651) × 3.57 = 9300.42 m s^{-1}

D**3** = (690 + 1160ρ_{03}) $\sum N$**3** = (690+1160 × 1.842) × 3.21 = 9073.77 m s^{-1}

P**1** = 1.092 ($\rho_{01} \sum N$**1**)^2 – 0.574 = 1.092 × (1.551 × 3.50)^2 - 0.574 = 31.61 Gpa

P**2** = 1.092 ($\rho_{02} \sum N$**2**)^2 – 0.574 = 1.092 × (1.651 × 3.57)^2 - 0.574 = 37.36 Gpa

P**3** = 1.092 ($\rho_{03} \sum N$**3**)^2 – 0.574 = 1.092 × (1.842 × 3.21)^2 - 0.574 = 37.60 Gpa

The calculated P and D of compounds are larger to that of TNT, while **2** and **3** are slightly larger than RDX.

3.8. Sensitivity test

The impact sensitivity was determined by using a Fall Hammer Apparatus. Twenty milligrams of compounds were compacted to a copper cap under the press of 39.2 MPa and hit by a 2 kg drop hammer, and calculated value of H_{50} represents the drop height of 50% initiation probability. The test result shows that the compounds don't fire at the highest point of 200 cm, which corresponds to the impact energy of 40 J. Under the same test condition, the impact sensitivity value (h_{50}) of TNT was 76.5 cm (15.0 J), which are consistent with the values from the reference [33]. Hence, the impact sensitivities of the compounds are lower than that of TNT.

Friction sensitivities of the compounds were measured by applying a Julius Peter's machine using 20 mg of the sample. No friction sensitivity was observed up to 36 kg. The friction sensitivities of the compounds are lower than that of RDX (12 kg). [34]

The results reveal that the compounds are insensitive to impact and friction stimulus. Physicochemical properties are listed in Table 5.

Table 5

4. Conclusions

In summary, three energetic compounds have been synthesized and characterized. X-ray analysis indicates that the stabilities of compounds are related to intermolecular interactions in the solid state. Specifically, **3** exhibits rarely structure, in which two nitrate anions interact with DAT in asymmetry unit. The superior thermostabilities of title compounds are present with high decompose temperature of 246 (the host framework), 185 and 245 ^{o}C, respectively. The standard molar enthalpies of formation for three compounds have been calculated to be 478.13, 382.56 and –346.63 kJ mol^{-1}, respectively. The sensitivity measurements indicate that compounds are insensitive to external stimuli. Calculated detonation values of compounds **2** and **3** are slightly higher than that of TNT and RDX. According to above results, the compounds behave as favorable potential of energy-rich materials.

Acknowledgements

We gratefully acknowledge the financial support from the National Natural Science Foundation of China (Grant Nos. 21373162, 21127004, 21173168 and 21203149), and the Nature Science

Foundation of Shaanxi Province (Grant Nos. 11JS110, FF10091 and SJ08B09).

Supporting Information

Selected bond lengths, bond angles and hydrogen bonds for compounds **1**-**3**.

Simulated and experimental powder X-ray diffraction patterns of compounds at room temperature.

References

1 (a) D. M. Badgujar, M. B. Talawar, S. N. Asthana, P. P. Mahulikar, *J. Hazard. Mater*., 2008, **151**, 289; (b) Q. Yang, S.-P. Chen, G. Xie, S.-L. Gao, *J. Hazard. Mater*., 2011, **197**, 199; (c) M. B. Talawar, R. Sivabalan, T. Mukundan, H. Muthurajan, A. K. Sikder, B. R. Gandhe, A. S. Rao, *J. Hazard. Mater*., 2009, **161**, 589; (d) D. Schmitt, P. Eyerer, P. Elsner, *Propellants, Explos., Pyrotech*., 1997, **22**, 109.

2 (a) A. V. Samet, V. N. Marshalkin, K. A. Lyssenko, V. V. Semenov, *Russ. Chem. Bull*., 2009, **58**, 347; (b) C. W. An, F.-S. Li, X.-L. Song, Y. Wang, X.-D. Guo, *Propellants, Explos., Pyrotech*., 2009, **34**, 400; (c) J. C. Oxley, J. L. Smith, J. Yue, J. Moran, *Propellants, Explos., Pyrotech*., 2009, **34**, 421.

3 (a) H.-W. Qiu, V. Stepanov, A. R. Di Stasio, T. Chou, W. Y. Lee, *J. Hazard. Mater*., 2011, **185**, 489; (b) A. S. Kumar, V. B. Rao, R. K. Sinha, A. S. Rao, *Propellants, Explos., Pyrotech*., 2010, **35**, 359.

4 (a) Y.-Q. Wu, L.-F. Huang, Hazard. *J. Hazard. Mater*., 2010, **183**, 324; (b) C.-W. An, J.-Y. Wang, W.-Z. Xu, F.-S. Li, *Propellants, Explos., Pyrotech*., 2010, **35**, 365; (c) C.-J. An, Y.-L. He, G.-H. Huang, Y.-H. Liu, *J. Hazard. Mater*., 2010, **179**, 526.

5 (a) H. Feuer, A. T. Nielsen, *Nitro Compounds*, Wiley-VCH, Weinheim, Germany, 1990; (b) A. T. Nielsen, *Nitrocarbons*, Wiley-VCH, Weinheim, Germany, 1995.

6 A. K. Sikder, N. Sikder, *J. Hazard. Mater*., 2004, **112**,1.

7 T. M. Klapötke, *Nachr. Chem. Tech*., 2008, **56**, 645.

8 H. Gao, J. M. Shreeve, *Chem. Rev*. 2011, **111**, 7377.

9 (a) T. M. Klapötke, C. M. Sabaté, *Chem. Mater.*, 2008, **20**, 3629; (b) T. M. Klapötke, P. Mayer, C. MiróSabaté, J. M. Welch, N. Wiegand, *Inorg. Chem*., 2008, **47**, 6014; (c) H. Xue, H. Gao, B.

Twamley, J. M. Shreeve, *Eur. J. Inorg. Chem*., 2006, **15**, 2959.

10 (a) K. E. Riley, M. Pitonak, P. Jurecka, P. Hobza, *Chem. Rev*., 2010, **110**, 5023; (b) R. Gutzler, O. Ivasenko, C. Fu, J. L. Brusso, F. Rosei, D. F. Perepichka, *Chem. Commun*., 2011, **47**, 9453.

11 (a) U. Bemm, H. stmark, *Acta Crystallogr., Sect. C*, 1998, **54**, 1997-1999; (b) H. H. Cady, A. C. Larson, *Acta Crystallogr*., 1965, **18**, 485.

12 T. M. Klapötke, P. Mayer, K. Polborn, *Chem. Mater*., 2008, **20**, 4519.

13 (a) T. M. Klapötke in *Moderne Anorganische Chemie*, 3rd ed. (Ed.: E. Riedel), Walter de Gruyter, Berlin, 2007, pp.99; (b) R. P. Singh, R. D. Verma, D. T. Meshri, J. M. Shreeve, *Angew. Chem. Int. Ed.,* 2006, **45**, 3584; (c) B. Rice, E. F. C. Byrd, W. D. Mattson in *High Energy Density Materials*(Ed.:T. M. Klapötke), Springer, 2007, pp. 153.

14 M. Eberspächer, T. M. Klapötke, C. Miró Sabaté, *Helvetica Chimica Acta*., 2009, **92**, 977.

15 (a) K. O. Christe, W. W. Wilson, J. A. Sheehy, J. A. Boatz, *Angew. Chem*., 1999, **111**, 2112. (b) D. E. Chavez, M. A. Hiskey, R. D. Gilardi, *Angew. Chem*., 2000, **112**, 1861; (c) Giles, J. *Nature*., 2004, **427**, 580. (d) H. Xue, S. W. Arritt, J. M. Shreeve, *Inorg. Chem*., 2004, **43**, 7972.

16 (a) R. P. Singh, R. D. Verma, D. T. Meshri, J. M. Shreeve, *Angew. Chem*., 2006, **118**, 3664; (b) T. Abe, G.-H. Tao, Y.-H. Joo, Y. Huang, B. Twamley, J. M. Shreeve, *Angew. Chem*., 2008, **47**, 6236; (c) M. A. Hiskey, N. Goldman, J. R. Stine, *J. Energ. Mater*., 1998, **16**, 119; (d) Y. Huang, H. Gao, B. Twamley, J. M. Shreeve, *Eur. J. Inorg. Chem*., 2008, **16**, 2560.

17 T. M. Klapötke, F. A. Martin, N. T. Mayr, J. Stierstorfer, *Z. Anorg. Allg. Chem*., 2010, **636**, 2555.

18 R. Meyer, J. Köhler (Eds.), *Explosives*, 4th ed. revised and extended, VCH Publishers, New York, 1993, 149.

19 R. Meyer, J. Köhler (Eds.), *Explosive*s, 4th ed. revised and extended, VCH Publishers, New York, 1993, 197.

20 M. J. Frisch, G. W. Trucks, H.B. Schlegel, G. E. Scuseria, M.A. Robb, J. R. Cheeseman, J. A. Montgomery, T. Vreven, K. N. Kudin, J. C. Burant, J. M. Millam, S. S. Iyengar, J. Tomasi, V. Barone, B. Mennucci, M. Cossi, G. Scalmani, N. Rega, G. A. Petersson, H. Nakatsuji, M. Hada, M. Ehara, K. Toyota, R. Fukuda, J. Hasegawa, M. Ishida, T. Nakajima, Y. Honda, O. Kitao, H. Nakai, M. Klene, X. Li, J. E. Knox, H. P. Hratchian, J. B. Cross, C. Adamo, J. Jaramillo, R.

Gomperts, R. E. Stratmann, O. Yazyev, A. J.Austin, R. Cammi, C. Pomelli, J. W. Ochterski, P. Y. Ayala, K. Morokuma, G. A.Voth, P. Salvador, J. J. Dannenberg, V. G. Zakrzewski, S. Dapprich, A. D. Daniels, M. C. Strain, O. Farkas, D. K. Malick, A. D. Rabuck, K. Raghavachari, J. B. Foresman, J. V. Ortiz, Q. Cui, A. G. Baboul, S. Clifford, J. Cioslowski, B. B. Stefanov, G. Liu, A. Liashenko, P. Piskorz, I. Komaromi, R. L. Martin, D. J. Fox, T. Keith, M. A. Al-Laham, C. Y. Peng, A. Nanayakkara, M. Challacombe, P. M. W. Gill, B. Johnson, W. Chen, M. W. Wong, C. Gonzalez, J. A. Pople, *Gaussian 03*. Revision B.01, Gaussian Inc., Pittsburgh, PA, 2003.

21 X.-W. Yang, S.-P. Chen, S.-L. Gao, *Instrum. Sci. Technol*., 2002, **30**, 311.

22 G. M. Sheldrick, *SHELXS-97*, Program for X-ray Crystal Structure Determination, University of Göttingen, Germany, 1997.

23 G. M. Sheldrick, *SHELXL-97*, Program for X-ray Crystal Structure Refinement, University of Göttingen, Germany, 1997.

24 N. Stanley, V. Sethuraman, P. T. Muthiah, P. Luger, M. Weber, *Cryst. Growth Des*., 2002, **2**, 631.

25 X. G. Zhang, *Master's Dissertation*, University of Defense Technology, Beijing, 2005.

26 H. E. Kissinger, Reaction kinetics in differential thermal analysis, *Anal. Chem*., 1957, **29**, 1702.

27 T. Ozawa, A new method of analyzing thermo-gravimetric data, *Bull. Chem. Soc. Jpn*., 1965**,** **38**, 1881.

28 C. D. J. Doyle, Kinetic analysis of thermo-gravimetric data, *J. Appl. Polym. Sci*., 1961, **5**, 285.

29 J. D. Cox, D. D. Wagman, V. A. Medvedev, *CODATA Key Values for Thermodynamics*. Hemisphere Publishing Corp: New York, 1989.

30 (a) H.-X. Chen, S.-S. Chen, L.-J. Li, Q.-Z. Jiao, T.-Y. Wei, S.-H. Jin, *J. Hazard. Mater*., 2010, **175**, 569; (b) Y.-H. Ren, W. Li, F.-Q. Zhao, J.-H. Yi, B. Yan, H.-X Ma, K.-Z. Xu, J.-R. Song, R.-Z. Hu, *J. Anal. Appl. Pyrol*., 2013, **102**, 89.

31 (a) O. S. Bushuyev, P. Brown, A. Maiti, R. H. Gee,G. R. Peterson, B. L. Weeks, L. J.Hope-Weeks, *J. Am. Chem. Soc*., 2012, **134**, 1422; (b) S.-H. Li, Y. Wang, C. Qi, X.-X. Zhao, J.-H. Zhang, S.-W. Zhang, S.-P. Pang, *Angew. Chem. Int. Ed*., 2013, **52**, 1.

32 Y. Guo, H. Zhang, *Explos. Shock Waves*., 1983, **3**, 5623.

33 J. Köhler, R. Meyer, in: *Explosivstoffe* 9th ed., Wiley-VCH, Weinheim, Germany,1998.

34 M. Anniyappan, M. B. Stalwart, G. M. Gore, S. Venugopalan, B. R. Gandhe, *J. Hazard. Mater.*, 2006**, 137**, 812.

Figure captions

Figure 1. (a) The asymmetric unit of **1** showing the part of atom-numbering scheme and intermolecular hydrogen bonds (shown as dashed lines). (b) The hydrogen bond modes of H_2O in **1**. (c) The hydrogen bond modes of TZA. (d) The 3D network of **1**.

Figure 2. (a) The asymmetric unit of **2** showing the part of atom-numbering scheme and intermolecular hydrogen bonds (shown as dashed lines). (b) The face-to-face of tetrazole cations alignment showing the π-π stacking interaction. (c) The 2-D layer in **2**.

Figure 3. (a) The asymmetric unit of **3** showing the part of atom-numbering scheme and intermolecular hydrogen bonds (shown as dashed lines). (b) DAT interacts with six nitrate anions. (c) The 2D layer in **3**.

Figure 4. DSC curves of compounds **1–3**.

Figure 5. TG curves of compounds **1–3**.

Figure 6. View of HOMO (left) and LUMO (right) for **1** by B3LYP/6-311+G(d).

Figure 7. View of HOMO (left) and LUMO (right) for **2** by B3LYP/6-311+G(d).

Figure 8. View of HOMO (left) and LUMO (right) for **3** by B3LYP/6-311+G(d).

Table 1. Crystal data and structure refinement details for compounds **1–3**.

Table 2. The peak temperatures of the exothermic processes at different heating rates and the thermokinetic parameters.

Table 3. Calculated parameters used in the detonation reactions.

Table 4. Nitrogen equivalents of different detonation products.

Table 5. Physicochemical properties of energetic compounds **1–3**.

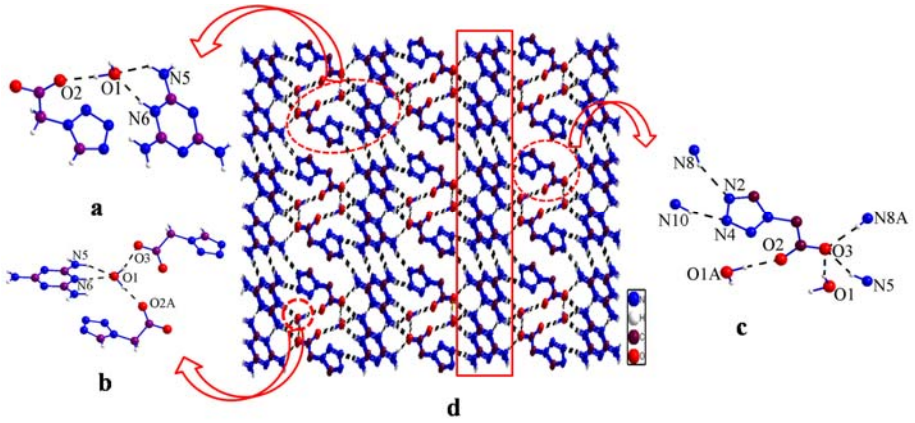

Figure 1. (a) The asymmetric unit of **1** showing the part of atom-numbering scheme and intermolecular hydrogen bonds (shown as dashed lines). (b) The hydrogen bond modes of H_2O in **1**. (c) The hydrogen bond modes of TZA. (d) The 3D network of **1**.

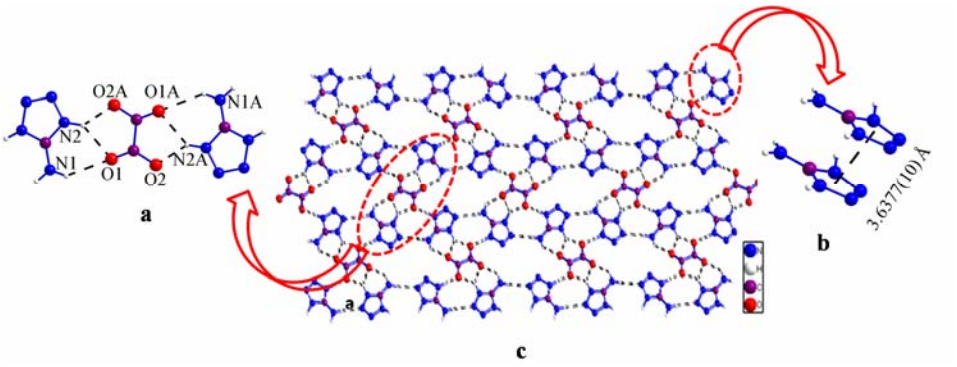

Figure 2. (a) The asymmetric unit of **2** showing the part of atom-numbering scheme and intermolecular hydrogen bonds (shown as dashed lines). (b) The face-to-face of tetrazole cations alignment showing the π-π stacking interaction. (c) The 2-D layer in **2**.

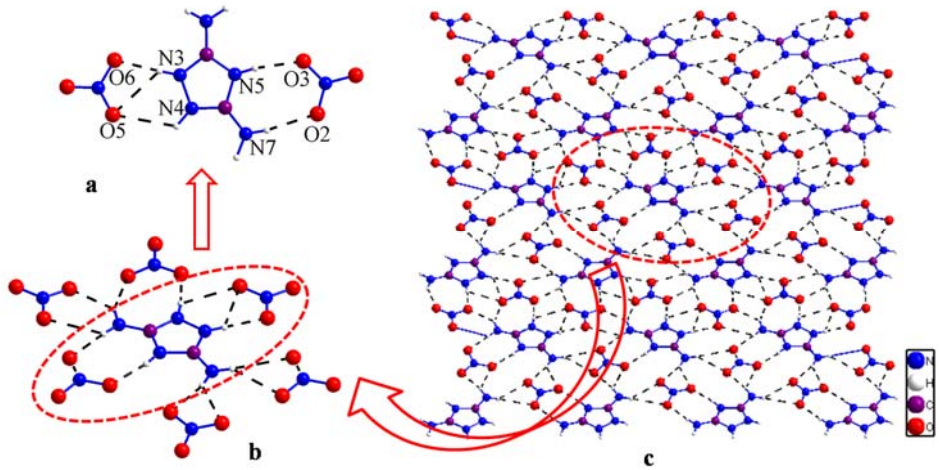

Figure 3. (a) The asymmetric unit of **3** showing the part of atom-numbering scheme and intermolecular hydrogen bonds (shown as dashed lines). (b) DAT interacts with six nitrate anions. (c) The 2D layer in **3**.

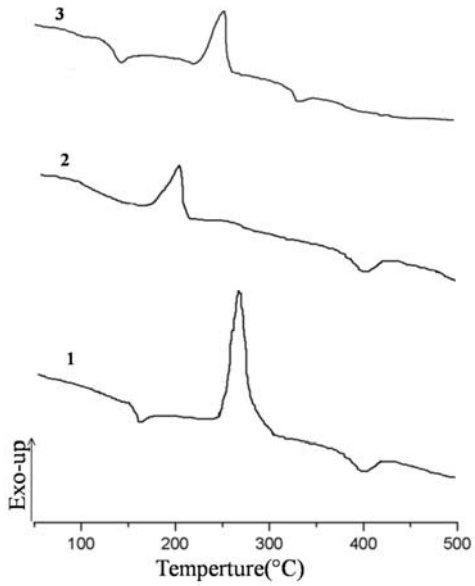

Figure 4. DSC curves of compounds **1–3**.

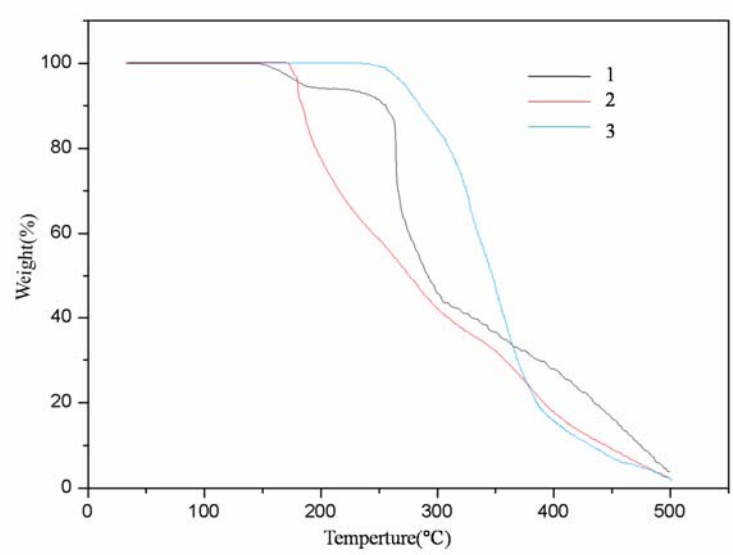

Figure 5. TG curves of compounds **1–3**.

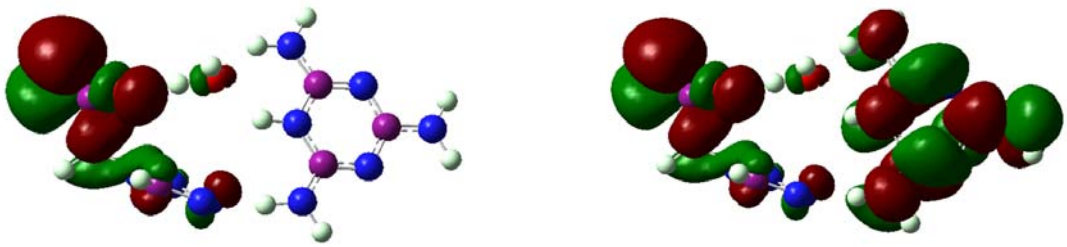

Figure 6. View of HOMO (left) and LUMO (right) for **1** by B3LYP/6-311+G(d).

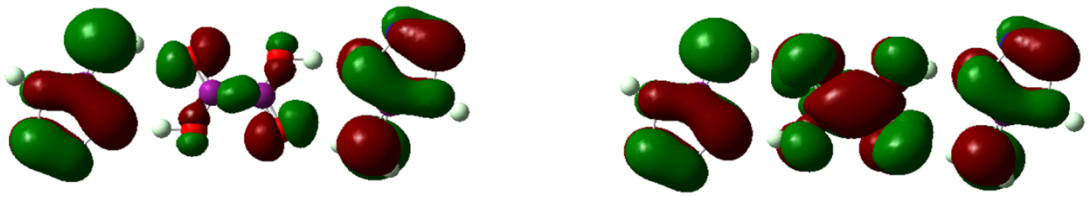

Figure 7. View of HOMO (left) and LUMO (right) for **2** by B3LYP/6-311+G(d).

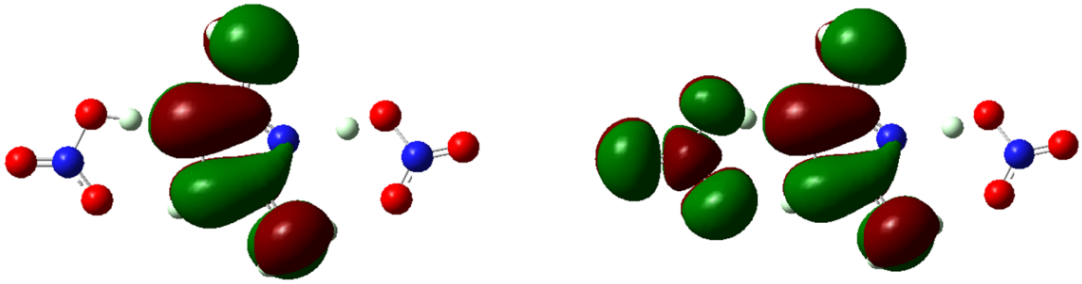

Figure 8. View of HOMO (left) and LUMO (right) for **3** by B3LYP/6-311+G(d).

Table 1. Crystal data and structure refinement details for compounds **1–3**.

Compound	**1**	**2**	**3**
Empirical formula	$C_6H_{12}N_{10}O_3$	$C_4H_8N_{10}O_4$	$C_2H_7N_7O_6$
Formula weight	272.26	260.20	225.15
Crystal system	Triclinic	Monoclinic	Monoclinic
space group	*P*-1	*P*2(1)/*c*	*P*2(1)/*c*
a (Å)	5.1633(11)	3.6377(10)	13.559(3)
b (Å)	9.5569(19)	11.723(3)	8.9163(17)
c (Å)	12.229(3)	12.387(3)	6.7232(13)
α (°)	87.326(3)	90	90
β (°)	83.816(3)	97.696(5)	93.051(4)
γ (°)	76.459(3)	90	90
V (Å^3)	630.89(12)	523.5(2)	811.7(3)
Z	2	2	4
F(000)	284	268	464
GOF on F^2	1.016	1.040	1.007
R indices (all data)	R_1 = 0.0839 wR_2 = 0.2373	R_1 = 0.0902 wR_2 = 0.1819	R_1 = 0.0674 wR_2 = 0.1099
Final *R* indices [*I*>2sigma(*I*)]	R_1 = 0.0667 wR_2 = 0.2099	R_1 = 0.0529 wR_2 = 0.1315	R_1 = 0.0430, wR_2 = 0.0970

Table 2. The peak temperatures of the exothermic processes at different heating rates and the thermokinetic parameters.

Compounds	**1**	**2**	**3**
Heating rate β (°C min^{-1})	Peaks temperatures T_p (°C)		
2	262.0	177.8	236.2
5	264.8	189.1	240.4
8	266.3	193.6	246.3
10	268.3	197.5	256.6
The calculation results by Kissinger's method			
E_k (kJ mol^{-1})	625.381	139.402	152.472
ln A_k(s^{-1})	59.024	13.584	13.160
Linear correlation coefficient (R_k)	0.9956	0.9962	0.9987
The calculation results by Ozawa–Doyle's method E_o (kJ mol^{-1})	603.211	139.839	153.211
Linear correlation coefficient (R_o)	0.9981	0.9985	0.9989

Table 3. Calculated parameters used in the detonation reactions.

Entry	Compounds (hartree)	H_2 (hartree)	CO (hartree)	N_2 (hartree)	C (hartree)	CO_2 (hartree)	H_2O (hartree)	ΔE_{det} (hartree)	ΔE_{det} (kcal g^{-1})	ΔH_{det} (kcal g^{-1})	ΔH_{det} (kcal cm^{-3})
1	-1009.0937	-1.1666	-113.341	-109.447	-37.738			1.6221	3.7386	4.2594	6.6063
2	-1005.6766	-1.1666	-113.341	-109.447				0.4112	0.9917	1.1636	1.9211
3	-914.8853		-113.341	-109.447		-188.629	-76.3776	0.1732	0.4827	0.5900	1.0868

Table 4. Nitrogen equivalents of different detonation products.

Detonation product	N_2	H_2O	CO	CO_2	O_2	C	H_2
Nitrogen equivalent index	1.00	0.54	0.78	1.35	0.50	0.15	0.29

Table 5. Physicochemical properties of energetic compounds **1–3**.

	1	2	3	TNT[31]	RDX[31]
formula	$C_6H_{12}N_{10}O_3$	$C_4H_8N_{10}O_4$	$C_2H_7N_7O_6$	$C_7H_5N_3O_6$	$C_3H_6N_6O_7$
Molecular Mass (g mol^{-1})	272.26	260.20	225.15	227.13	222.12
Impact sensitivity (J)[a]	>40	>40	>40	15	7.5
Friction sensitivity (N)[b]	>360	>360	>360	353	120
N (%)[c]	51.42	53.80	43.53	18.50	37.80
Ω (%)[d]	–88.15	–49.15	–10.66	–73.96	–21.60
T_{dec} (°C)[e]	246	185	245	>160	210
ρ_0 (g cm^{-3})[f]	1.551	1.651	1.843	1.654	1.800
$\Delta_f H_m^{\theta}$ (kJ mol^{-1})[g]	478.13	382.56	-346.63	59.1	70
ΔH_{det} (kcal g^{-1})[h]	4.2594	1.1636	0.5900	1.22	1.44
P (GPa)[i]	31.61	37.36	37.60	20.5	34.1
D (m s^{-1})[j]	8712.06	9300.42	9073.77	7178	8906

[a] Impact sensitivity. [b] Friction sensitivity. [c] Nitrogen content. [d] Oxygen balance. [e] Decomposition temperature. [f] From X-ray diffraction. [g] Calculated energy of formation. [h] Energy of explosion. [i] Detonation pressure. [j] Detonation velocity.